Received: 1 March 2023 | Revised: 13 November 2023 | Accepted: 30 November 2023
DOI: 10.1002/hyp.15055

RESEARCH ARTICLE

WILEY

The turning of ecological change in the Yellow River Basin

Tonghui Gu[1] | Xiaodan Guan[1,2] | Jianping Huang[1,2] | Xiaohan Shen[1] | Xiaoqian Huang[1] | Guolong Zhang[2] | Dongliang Han[2] | Li Fu[1] | Junsheng Nie[3]

[1]Key Laboratory for Semi-Arid Climate Change of the Ministry of Education, College of Atmospheric Sciences, Lanzhou University, Lanzhou, China

[2]Collaborative Innovation Center for Western Ecological Safety, Lanzhou University, Lanzhou, China

[3]Key Laboratory of Western China's Environmental System (Ministry of Education), College of Earth and Environmental Sciences, Lanzhou University, Lanzhou, China

Correspondence
Xiaodan Guan, Key Laboratory for Semi-Arid Climate Change of the Ministry of Education, College of Atmospheric Sciences, Lanzhou University, Lanzhou, China.
Email: guanxd@lzu.edu.cn

Funding information
"Innovation Star" Project for Outstanding Postgraduates of Gansu Province, Grant/Award Number: 2023CXZX-105; Fundamental Research Funds for the Central Universities, Grant/Award Number: lzujbky-2022-ct06; National Natural Science Foundation of China, Grant/Award Numbers: 42041004, 41991231

Abstract

The Yellow River Basin (YRB) as a source of the oldest world cultures, flows through vast arid and semi-arid regions of China. Its fragile vegetation is suffering the obvious effect from regional climate change, and easily turns from a critical state into qualitatively different modes of change, which implies significant impacts on humans and ecosystems. Our results show that in the period of 1982–2015, the normalized difference vegetation index (NDVI) appeared significantly discontinuous changes by stagnant warming and strengthening wetting, especially in the central YRB (104.5°–111° E, 35.5°–38° N). The NDVI in this region shifted from slowly increasing (5.42×10^{-4} a^{-1}) to rapidly increasing (5.13×10^{-3} a^{-1}) around 2003, called the turning point (TP). Such shift change is mainly a result of increased moderate rain, with frequency trend changed from 0.083 times·a^{-1} to 0.324 times·a^{-1}. Meanwhile, these changes on vegetation led to a reversal of the gross primary productivity (GPP) from decreasing to increasing. Such results indicated the vulnerable ecosystem of the central YRB has played a positive contribution to the carbon balance, and more sustainable management of vegetation is required for the ecological development and engaging adaptive strategy.

KEYWORDS
GPP, moderate rain, NDVI, piecewise linear regression, Yellow River Basin

1 | INTRODUCTION

Vegetation is an important component of the land-atmosphere system (Fu et al., 2014; Liu et al., 2019; Piao et al., 2015; Zhao et al., 2020). On the one hand, the growth of vegetation is strongly affected by climate change (Fu et al., 2021; Jiang et al., 2014; Xu et al., 2013); on the other hand, the growth of vegetation also affects climate through various complex physical and biological processes (Li, Zhang, et al., 2020; Li, Li, et al., 2020; Liu et al., 2005; Peng et al., 2014). "Vegetation greening" is defined as statistically significant increase in annual or seasonal vegetation greenness at a location (Piao et al., 2020). A growing number of studies have shown that the Earth has experienced an unprecedented trend of vegetation greening since the 1980s (Fensholt et al., 2009; Kumar et al., 2020), especially in the northern temperate regions (Chen et al., 2019; Piao et al., 2020; Tian et al., 2021). The Yellow River Basin (YRB) is located in the northern temperate region of China, most of which are arid and semi-arid regions (Huang et al., 2020). The YRB as an important ecological barrier in northern China, its vegetation cover is subject to complex changes under the effects of both climatic factors and human activities, resulting in a very fragile ecological environment (Chen et al., 2022; Guan et al., 2019; Liu & Randerson, 2008). Therefore, conducting a quantitative analysis of how climate and ecology changed in the YRB in recent decades when vegetation changed holds significant importance for formulating regional climate regulation policies and ecological conservation efforts (Yang et al., 2016; Zhao et al., 2019).

The normalized difference vegetation index (NDVI) is a remotely sensed vegetation index widely used to indicate vegetation greenness. Because the NDVI has strong correlations with vegetation coverage, it is widely used to detect and attribute vegetation greening trend (Liu et al., 2019; Piao et al., 2011). As an important tool to study vegetation change, remote sensing monitoring of vegetation can accurately reflect the dynamic change of vegetation in vast areas, and has become one of the important tools in global climate change research (Ukkola et al., 2021; Xin et al., 2008; Xu & Yang, 2014). Recent studies have indicated the emergence of critical turning point (TP) in the trend of terrestrial vegetation change, which is a crucial threshold at which small quantitative changes lead to significant qualitative changes, once the magnitude of climate change exceeds the critical value, irreversible effects will occur and the regional ecology will be out of balance (Lenton et al., 2008; Li et al., 2023; Liu et al., 2023). For instance, in Central Asia, vegetation has exhibited browning since 1997 due to declining soil moisture (Yao, Gao, et al., 2021; Yao, Mao, et al., 2021). Similarly, in the early 1990s, vegetation in the northwestern region of North America underwent a browning trend attributed to cooling during spring and summer (Wang et al., 2011). These phenomena have contributed to unfavourable ecological impacts such as exacerbated droughts and heightened ecosystem instability. However, the presence of a critical TP in the YRB's vegetation and the trends on either side of this threshold remain uncertain.

In recent decades, the YRB has shown a warm and dry trend (Ma et al., 2020), and the NDVI is also experiencing a greening trend (Kong et al., 2016; Piao et al., 2020). But previous studies often focused on the last four decades; and these studies concluded that the increase in temperature dominated the increase in the NDVI in the YRB (Toms & Lesperance, 2003; Wang et al., 2011). Some studies showed that while changes in vegetation cover are also affected by urbanization, the areas controlled by precipitation increased significantly in the recent past (Sun et al., 2021; Yuan et al., 2020). However, in the context of global climate change, vegetation cover has been changing in a complex way in recent decades, and the trend even reverses in some regions (Feng et al., 2021; Jiang et al., 2021; Wang et al., 2011). National policies such as The Grain for Green Program also played a key role in this process (Chen et al., 2016; Hou et al., 2022; Yu et al., 2022). Hence, it is imperative to explore how vegetation greening has transformed in the YRB and to comprehend the causes behind the occurrence of this transformation.

Vegetation effectively controls the carbon exchange between the land and atmosphere, so changes in vegetation have a great effect on the ecosystem carbon balance (Jamali et al., 2015; Yao et al., 2019; Yuan et al., 2022). Since 2020, the "Double Carbon" target has been known as a national strategy in China (Xi et al., 2019). Vegetation growth in China plays an extremely important role in the global carbon cycle (Yao et al., 2020). Over the past decades, vegetation in China absorbed approximately 28%–37% of China's fossil fuel emissions, contributing to a net accumulation of 0.18–0.26 Pg/a of carbon (Piao et al., 2009; Piao et al., 2014). Gross primary productivity (GPP) is the carbon flux fixed in terrestrial ecosystems by organisms (mainly green plants) from the atmosphere through photosynthesis, which can accurately reflect changes in biomass; so it is widely used to assess the carbon storage capacity of ecosystems (Gui et al., 2021; Hou et al., 2022; Zhou et al., 2019). In recent years, a number of studies have investigated carbon exchange between terrestrial ecosystems and atmosphere on hemispheric scale by using GPP, but little

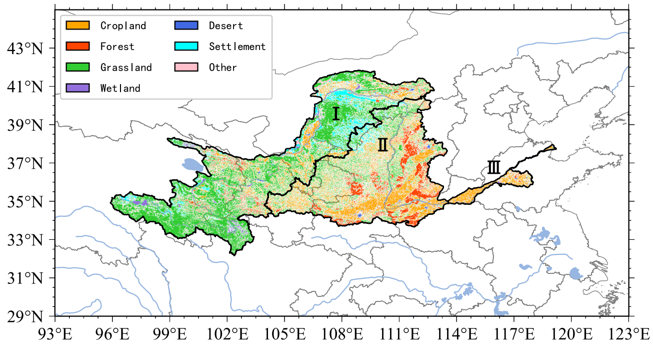

FIGURE 1 Locations and terrestrial ecosystem types of the upper (I), middle (II), and lower (III) reaches of the YRB in 2015.

attention has been given to the specificity of regional carbon exchange (Tang et al., 2022; Zhang, Gentine, et al., 2022; Zhang, Li, et al., 2022; Zhang, Piao, et al., 2022). As an important ecological reserve in northern China, the YRB is now a key area for the development of green economy; thus, gaining an understanding of how regional carbon storage capacity changes amidst the shift in vegetation greening trends is of utmost importance (Feng et al., 2016; Kong et al., 2016).

The objective of this study is to detect the TP of the regional-scale vegetation changes and investigate the changes in both NDVI and carbon on either side of the TP across the YRB. The rest of the paper is organized as follows. In Section 2, we introduce the study area, datasets, and methods used in this study. In Section 3, we present the main results on the discontinuous change in the NDVI, its climatic causes, and the corresponding change in GPP from 1982 to 2015. In Sections 4 and 5, conclusion and discussion are given, respectively. The analysis conducted in this study focuses on addressing the following questions:

1. Whether there was a TP of NDVI trend in the YRB, and how the trend changed on both sides of the TP.
2. What were the climate drivers underlying the occurrence of the TP of NDVI trend in the YRB?
3. How did the carbon sequestration capacity of the YRB change under the background of the occurrence of the TP?

2 | MATERIALS AND METHODS

2.1 | Study area

The YRB covers the regions in 30°–45° N and 95°–120° E, with about 7.95×10^5 km^2; and the main river length is about 5464 km. The topography gradually descends from west to east, passing through the Tibetan Plateau, Inner Mongolia Plateau and Loess Plateau, eventually reaching the lower alluvial plains in a stepwise style. Furthermore, a majority of the YRB falls under the arid and semi-arid regions. To provide a more accurate description of the regional NDVI characteristics in the YRB, we partitioned the YRB into three sections based on the scheme proposed by the Yellow River Conservancy Commission of the Ministry of Water Resources (Figure 1): upper, middle and lower reaches. The section from the source to Hekou Town in the Inner Mongolia Autonomous Region is the upper reaches of the YRB, with the length of about 3472 km and an area of about 4.28×10^5 km^2. The section from Hekou Town to Taohuayu Village in Zhengzhou, Henan Province is the middle reaches of the YRB, with the length of about 1206 km and an area of 3.44×10^5 km^2. The section from Taohuayu Village to the Bohai Sea is the lower reaches of the YRB, with the length of 786 km and an area of only 2.3×10^4 km^2 (Zhang & Liu, 2020).

2.2 | Data

2.2.1 | NDVI data

The NDVI is defined as the ratio of the difference between near-infrared reflectance and red visible reflectance to the sum of the two, namely, (NIR-R)/(NIR + R), where NIR and R are near-infrared and red surface reflectance values, respectively (Jiang et al., 2021; Myneni et al., 1997; Sun et al., 2021). The NDVI data is from the Global Inventory Monitoring and Modelling Study (GIMMS) group, covering the period of 1982 to 2015, at 8-km resolution biweekly (Tucker et al., 2005). With relatively wide spatial coverage and long time span, this dataset has been widely used to detect changes in vegetation growth due to its reliability (Jiang et al., 2022; Nemani et al., 2003; Wei et al., 2022; Zhang, Gentine, et al., 2022; Zhang, Li, et al., 2022; Zhang, Piao, et al., 2022). The larger 15-day NDVI for a month was used to produce monthly NDVI data; and the data with NDVI<0.1 were treated as bare soil and removed (Wang et al., 2011; Yuan et al., 2020). In the following, the NDVI is synthesized as annual average for trend analysis and TP detection, etc.

2.2.2 | Climate data

The monthly precipitation, 2 m air temperature, soil moisture (0–7 cm) data used in this study are from the European Centre for Medium-Range Weather Forecasts (ECMWF) fifth generation atmospheric reanalysis (ERA5), which covers our study period of 1982–2015 (Lei et al., 2021; Pang et al., 2021). The ERA5 data has a resolution of $0.25^\circ \times 0.25^\circ$. We also used daily precipitation data from National Oceanic and Atmospheric Administration (NOAA) Climate Prediction Center (CPC) for calculating the frequency of rain, with a spatial resolution of $0.5^\circ \times 0.5^\circ$; the time period is 1982–2015 (Chen et al., 2002; Fan & Van den Dool, 2008). To verify the robustness of precipitation trend, we used the Global Precipitation Climatology Center (GPCC) data from 1982 to 2015 (Figure S1 in Supporting Information S1). With a temporal resolution of monthly and a spatial resolution of $0.25^\circ \times 0.25^\circ$, the GPCC data is widely used to estimate precipitation in the Northern Hemisphere (Huang et al., 2022; Zhu, Guan, et al., 2021; Zhu, Xiao, et al., 2021). In the following, climate data is synthesized as annual average for trend analysis, etc.

2.2.3 | GPP data

The GPP data is from the National Qinghai-Tibetan Plateau Data Center. The GPP data from 1982 to 2018 is based on remotely sensed NOAA Advanced Very High Resolution Radiometer (AVHRR) data and hundreds of flux stations in the world. The temporal resolution is monthly, and the spatial resolution is $0.05^\circ \times 0.05^\circ$. The GPP data units are gC·m^{-2} (Wang et al., 2021).

2.2.4 | Terrestrial ecosystems data

The Resource and Environment Science and Data Center (RESDC) is a terrestrial ecosystem types status database in China, with a spatial resolution of 1 km × 1 km and a time span of 7 years including 1980, 1990, 1995, 2000, 2005, 2010, and 2015 (Liu et al., 2022; Song et al., 2020; Zhu, Guan, et al., 2021; Zhu, Xiao, et al., 2021). Terrestrial ecosystems include seven primary types: cropland ecosystem, forest ecosystem, grassland ecosystem, wetland ecosystem, desert ecosystem, settlement ecosystem, and the other ecosystem.

2.3 | Trend analysis with piecewise linear regression method

To investigate whether the NDVI has a TP and what its effects are throughout the study period from 1982 to 2015, we applied a piecewise linear regression method to examine the time series of the NDVI at each grid point in the YRB. Specifically, the piecewise linear regression method attempts to find one or more TPs and performs a linear fit before and after each TP, so that the TP and its slope with the smallest sum of squares of the fitted residuals are the optimal solution of the piecewise linear regression (Toms & Lesperance, 2003). In particular, the model with only one TP is given by Equation (1) below.

$$y = \begin{cases} \beta_0 + \beta_1 t + \varepsilon, t \le \alpha \\ \beta_0 + \beta_1 t + \beta_2 (t - \alpha) + \varepsilon, t > \alpha, \end{cases} \tag{1}$$

where y is the NDVI; β_0, β_1 and β_2 are the regression coefficients; t is the year; α is the TP of the NDVI trend; and ε is the residual. The linear trend of the NDVI is β_1 before the TP, and is $\beta_1 + \beta_2$ after the TP. α is determined by the least squares method. We also restricted α to the period between 1986 and 2011 to avoid performing linear regressions in a period with too few data points (Tomé & Miranda, 2004; Wang et al., 2011).

To test the significance of the TP, we focus on three aspects as follows: (1) whether the residual plot is random; (2) comparing the difference between simple and piecewise regressions; and (3) comparing the slopes of the two sides of the TP to see whether there is a

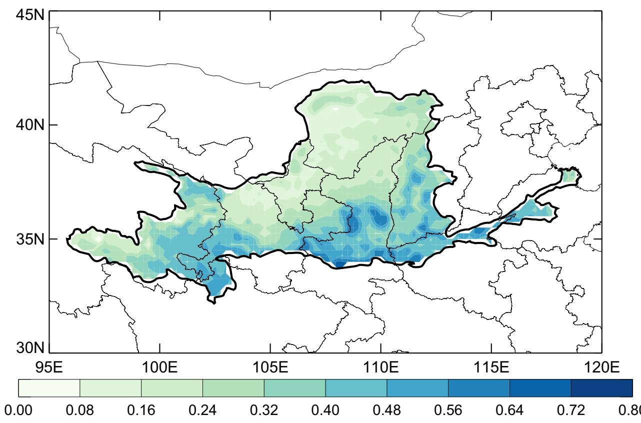

FIGURE 2 Spatial distribution of annual average NDVI in the YRB during 1982–2015.

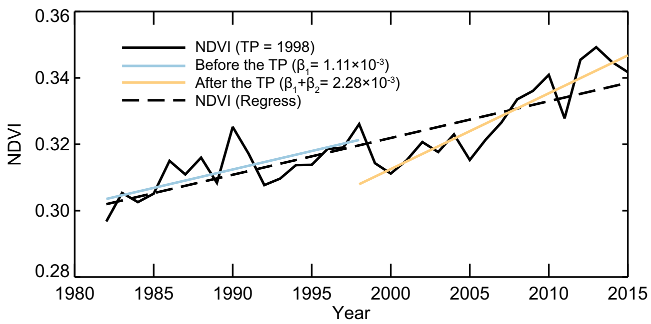

FIGURE 3 Trends in annual average NDVI in the YRB during the period of 1982–2015. The blue line is the regression before the TP. The yellow line is the regression after the TP. And the dashed line is the regression during the whole study time period.

significant difference (Shea & Vecchione, 2002). Therefore, we test the significance of the TP at each grid point in two ways (Wang et al., 2010) as follows.

1. Constructing an F-statistic for hypothesis testing, and calculating the F-statistic using Equation (2).

$$F = \frac{(RSS_{sl} - RSS_{pl})}{RSS_{pl}/(n-3)}, \tag{2}$$

where RSS_{sl} is the residual sum of squares of simple linear regression, RSS_{pl} is the residual sum of squares of piecewise linear regression, and n is the sequence length. The null hypothesis (H_0) is that there is no piecewise trend. The p-value of the TP is obtained by using the F-statistic; the H_0 hypothesis is rejected at $p < 0.05$, and the TP is considered significant.

2. Detect the abrupt change of trend. If there is any transformation between the three states of significant increase, significant decrease, and insignificant change before and after the TP, we also consider that the TP is significant. Here, the t-test is used to test the significance of the change at each side. A p-value<0.05 is considered significant (Weisberg, 2005). The Mann-Kendall test serves as an additional validation of the piecewise linear regression method, reinforcing the credibility of our results (Figure S2 in Supporting Information S1).

3 | RESULTS

3.1 | NDVI changes with respect to the TP

Figure 2 shows the spatial distribution of average NDVI from 1982 to 2015. Overall, the vegetation cover of the YRB was distributed in strips, rising from northwest to southeast. The source region was located in high-altitude cold area with widespread grassland ecosystem, while the vegetation cover in the northwestern part of the YRB was low, and mainly distributed in settlement ecosystem. The vegetation cover in the middle reaches was more vigorous, with a mixture of grassland ecosystem, forest ecosystem, and cropland ecosystem. The vegetation cover in the lower reaches was high with cropland ecosystem (Figures 1 and 2).

Figure 3 shows the time series of annual average NDVI in the YRB from 1982 to 2015, which had an abrupt change in 1998, called the TP. The trend of the NDVI during 1982–1998 was 1.11×10^{-3} a^{-1}, showing the vegetation in YRB increased before the TP. The rate of vegetation growth was more than doubled after 1998 (2.28×10^{-3} a^{-1}). The difference between the trends before and after the TP is significant, indicating that the TP is important to understand the change of the NDVI.

Figure 4a shows the spatial distribution of NDVI trend during 1982–2015 in the YRB. The NDVI displayed an increase in 92.5% of the YRB, with 76.8% exhibiting a significant increase, with an average value of 1.13×10^{-3} a^{-1}; and the trend was large than 4.00×10^{-3} a^{-1} in the middle and lower reaches of the YRB. Conversely, the NDVI displayed a decrease in only 7.5% of the YRB, with 4.0% exhibiting a significant decrease and a fragmented distribution across the YRB. As shown in Figure 4b, each grid point in the YRB has a TP for the NDVI trend, which spread over the 20-year period from 1990 to 2010, and most of them passed the significance test (94.8%). A noteworthy observation was that the TP of NDVI trend in the junction of the upper and middle reaches was after 2001, and dominated by settlement ecosystem with low vegetation cover (Figures 1 and 2). Whereas the source region, the lower reaches and southeastern of the middle reaches, which TP before 2001 have high vegetation cover. Furthermore, the NDVI in these three regions experienced an increasing trend before the TP, and a decreasing trend more recently. In contrast, the NDVI in the junction of the upper and middle reaches of the YRB increased slowly before the TP and quickly afterward (Figures 4c,d). Overall, the NDVI in about 88.7% of the YRB (46.2% with a significant increase) increased before the TP, and the average trend was 1.91×10^{-3} a^{-1}. After the TP, the NDVI displayed an increase in

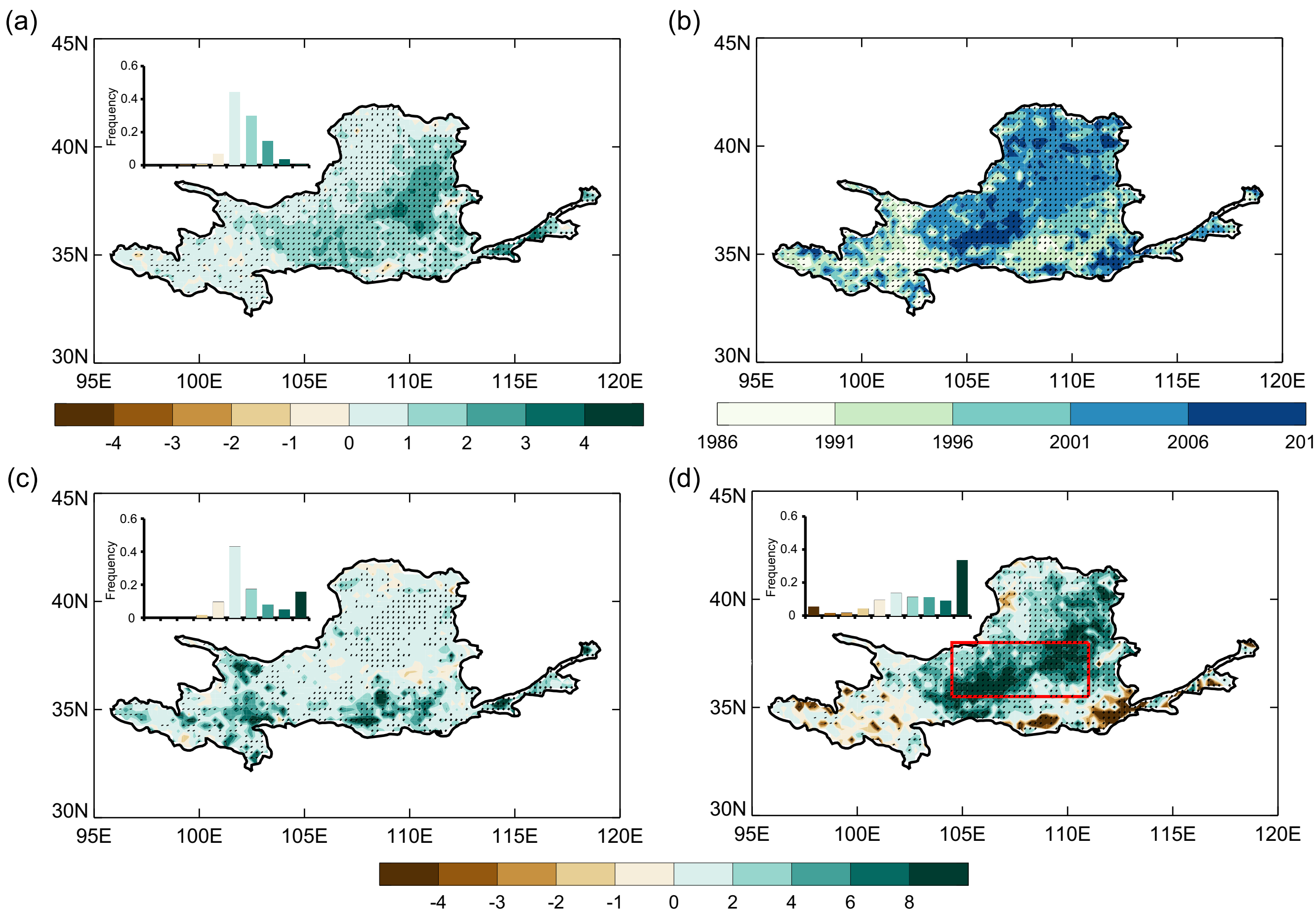

FIGURE 4 Spatial distribution of NDVI changes in the YRB. (a) NDVI trend during 1982–2015, (b) the year corresponding to the TP of NDVI trend, (c) NDVI trend before the TP, and (d) NDVI trend after the TP. The units of the NDVI trend is 10^{-3} a^{-1}. The small graphs in the upper left corner of (a), (c) and (d) show the frequency distributions of corresponding trends. Stippling indicates passing the significance test (p < 0.05).

78.1% of the YRB, with 57.2% exhibiting a significant increase. Remarkably, a frequency as high as 33.5% was observed for NDVI trend surpassing 8.00×10^{-3} a^{-1}, and the trend of the whole YRB remained at 2.64×10^{-3} a^{-1}. These results indicate that the increase in the high-value area of the growth trend was located in the central YRB (104.5°–111° E, 35.5°–38° N), with an average of 5.13×10^{-3} a^{-1} (only 5.42×10^{-4} a^{-1} before the TP; Figure 7c), which increased the NDVI of the whole YRB by cancelling out the decrease in the rest of the basin. It is worth noting that the regional average TP of the central YRB is 2003, and this TP will be used for subsequent regional average NDVI trend analysis.

3.2 | Temperature and precipitation changes with respect to the TP

Temperature and precipitation are climate factors closely related to the growth of vegetation, and therefore indispensable for analysing vegetation response to climate change (He et al., 2015; Kong et al., 2017; Sun et al., 2021; Wang et al., 2011). In the context of global warming, temperature increased over the entire YRB (99.2% with a significant increase) from 1982 to 2015, by 0.045°C·a^{-1} on average. The source region and the middle reaches warmed up the most, which reached 0.050°C·a^{-1} or more (Figure 5a). Before the TP, 95.3% of the YRB warmed up (69.5% with significant warming); and the warming was more dramatic compared to that of the entire study period (with an overall trend of 0.074°C·a^{-1}; Figure 5b). Similarly, the most significant warming trend can be seen in the source region and the middle reaches, more than 0.100°C·a^{-1}. Although some grid points showed a decreasing trend in temperature, none of them passed the significance test. After the TP, the YRB showed a stagnant warming trend or even a cooling trend, but the temperature still increased with a trend of 0.039°C·a^{-1} on average (Figure 5c). The frequency of warming trend greater than 0.025°C·a^{-1} before the TP was 95.2%, but only 44.2% after the TP. Especially, the central YRB showed a widespread cooling (48.3%) relative to before, decreasing from 0.081 to −0.006°C·a^{-1}, which is −0.073 times lower than the trend before the TP (Figure 6a,b). The cooling was not conducive to the growth of vegetation, contrary to the NDVI increasing in the central YRB (Angert et al., 2005; Fu et al., 2015).

From 1982 to 2015, precipitation displayed a decrease in 83.6% of the YRB, with 19.6% exhibiting a significant decrease and an average value of $-2.12\ \mathrm{mm \cdot a^{-1}}$; it showed a warm and dry trend (Ma et al., 2020), mainly in the eastern part of the YRB (Figures 5a,d). The northeastern and southern parts of the middle reaches, and the western part of the lower reaches showed the largest decreasing trend, which reached more than $-4.00\ \mathrm{mm \cdot a^{-1}}$. There was a slight increasing trend of precipitation in the source region, which may indicate the warming and wetting in the northwest in recent decades (Shi et al., 2003). However, there were distinct changes in precipitation before and after the TP of the NDVI. Before the TP, precipitation increased in the upper and lower reaches of the YRB, while it decreased in the middle reach (Figure 5e). After the TP, some regions showed opposite trends; for example, the lower reach and the source region showed a decreasing trend in the recent past, while the northeastern part of the middle reaches showed an increasing trend. Figures 5f and 6 clearly show that precipitation increased rapidly in the central YRB, with the trend increasing from $0.905\ \mathrm{mm \cdot a^{-1}}$ before 2003 to $5.203\ \mathrm{mm \cdot a^{-1}}$ afterwards (5.747 times), which is of great interest as it corresponded to the recent increase in the NDVI. Note that the precipitation showed a decreasing trend during 1982–2015 (Figure 5d) but increasing trends both before and after the TP (Figure 5e,f) for the central YRB. This inconsistency was caused by the high precipitation in 2003 and the sharp decline in 2004 (Figure S3 in Supporting Information S1). The results of the GPCC data is consistent with ERA5 before and after the TP (the correlation coefficients are 0.93 and 0.89, respectively), and showed a significant increase in precipitation trend after the TP, indicating that this result is reliable and adds our confidence to further explore the effect of precipitation on the NDVI (Figure S1c in Supporting Information S1).

3.3 | Moderate rain and soil moisture (0–7 cm) changes after the TP

According to the China Meteorological Administration (http://www.cma.gov.cn/), the intensity of rain can usually be classified into three levels, light rain ($0.1–10\ \mathrm{mm \cdot d^{-1}}$), moderate rain ($10–25\ \mathrm{mm \cdot d^{-1}}$), and heavy rain ($25–50\ \mathrm{mm \cdot d^{-1}}$). Moderate rain was found to be the most favourable type for vegetation growth (Figures 4d and 7a, and Figure S4 in Supporting Information S1). About 28.9% of the YRB showed a decreasing trend in the frequency of moderate rain (6.3% with a significant decrease), mainly in the source region, lower reaches, and northwestern part of the YRB, corresponding to the spatial distribution of the NDVI (Figure 4d). Similarly, about 71.1% of the YRB showed an increasing trend in moderate rain frequency (11.7% with a significant increase), especially in the central YRB where the average value reached $0.324\ \mathrm{times \cdot a^{-1}}$ ($0.083\ \mathrm{times \cdot a^{-1}}$ before the TP; Figures 7c and S5 in Supporting Information S1), much higher than the basin average ($0.087\ \mathrm{times \cdot a^{-1}}$).

Infiltration is a major component of precipitation expenditure component; its intensity is often expressed in terms of soil moisture. The root system usually absorbs water from the soil for vegetation growth and development; therefore, soil moisture affects vegetation growth condition (Fu et al., 2022; Loik et al., 2004). For moderate rain, the depth of infiltration is low and water will be confined to a shallow soil layer. Therefore, the moisture in the shallow soil layer of the central YRB also showed an increasing trend as the moderate rain increased (Figure 7b). Vegetation type in the central YRB was mainly grassland (Figure 1) with shallow root system, and thus can better absorb water in the shallow soil layer. In general, the spatial distribution of soil moisture trend in the YRB after the TP is similar to

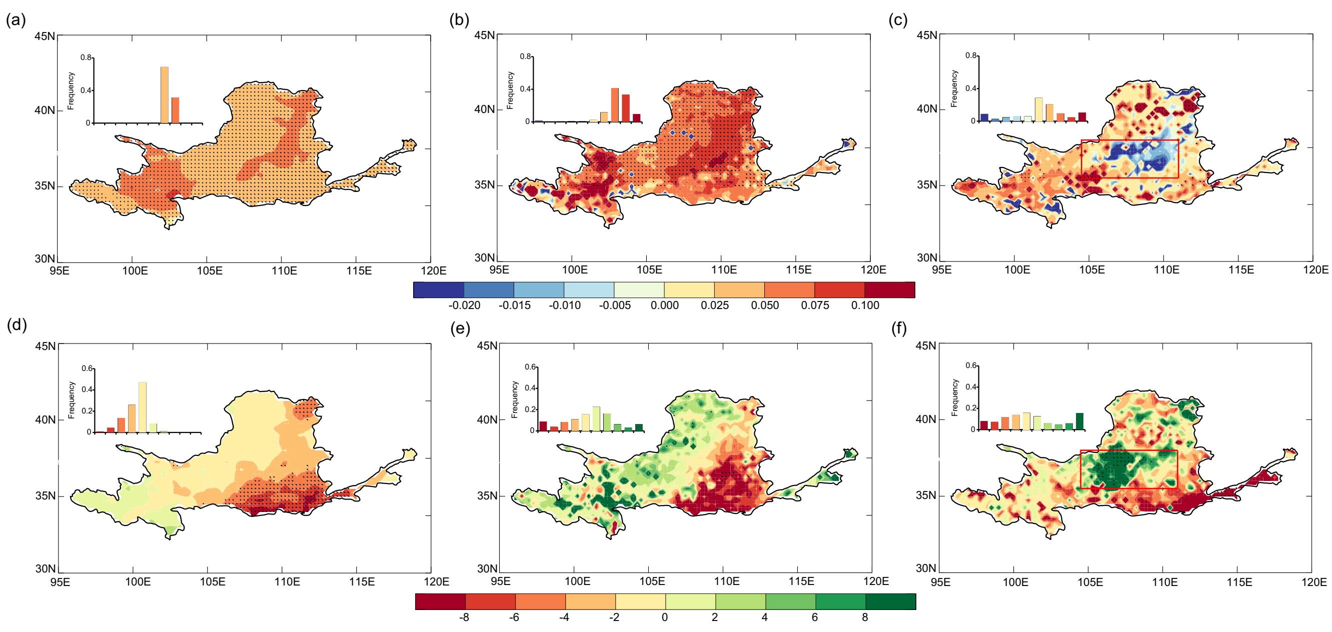

FIGURE 5 Spatial distribution of temperature trends (a) during 1982–2015, (b) before the TP, and (c) after the TP in the YRB (units: $^{\circ}\mathrm{C \cdot a^{-1}}$). Spatial distribution of precipitation trends (d) during 1982–2015, (e) before the TP, and (f) after the TP (units: $\mathrm{mm \cdot a^{-1}}$). The small graphs in the upper left corner show the frequency distributions of corresponding trends. Stippling indicates passing the significance test (p < 0.05).

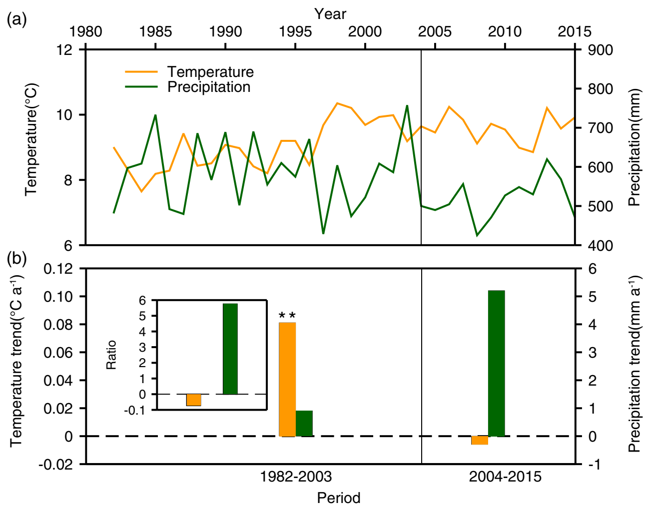

FIGURE 6 Interannual variations of temperature and precipitation in the central YRB during the periods of 1982–2003 and 2004–2015. (a) The variations of temperature (orange) and precipitation (green). (b) Trends of temperature and precipitation during 1982–2003 and 2004–2018. The small panel in the upper left corner of (b) shows the ratio of trends in temperature and precipitation in the later and earlier periods. ** indicates passing the significance test ($p < 0.01$). For visual clarity, the black vertical line in the figure is the dividing line with 2004 as the boundary.

that of moderate rain frequency. Especially in the central YRB where soil moisture increased (1.19×10^{-3} $m^3 \cdot m^{-3} \cdot a^{-1}$) with the frequency of moderate rain, the absorbable water increased in the grassland, the growth condition became better and better, and the NDVI increased ($R_{M\text{-}N} = 0.67$; Figure 7d) (Loik et al., 2004; Marone & Pol, 2021; Niu et al., 2021). Note that although moderate rain effectively suppressed the inhibitory effect of the cooling on vegetation growth, it essentially did not change the vegetation type (Figures 1 and S6 in Supporting Information S1).

3.4 | GPP changes with respect to the TP

Different with the NDVI, which is used to describe vegetation coverage, GPP represents the total influx of carbon into the ecosystem from the atmosphere and is typically used to describe regional carbon balance (Cheng et al., 2017; Lu et al., 2022; Yao, Gao, et al., 2021; Yao, Mao, et al., 2021; Yu et al., 2013). Figure 8c shows that the GPP displayed an increase in 74.1% of the YRB, with 39.8% exhibiting a significant increase, distributing in the source region and the western part of the middle reaches. The frequency distribution of GPP trend within the −2 to 2 $gC \cdot m^{-2} \cdot a^{-1}$ range accounts for a substantial 87.9%, with an average GPP trend of 1.6 $gC \cdot m^{-2} \cdot a^{-1}$. Conversely,

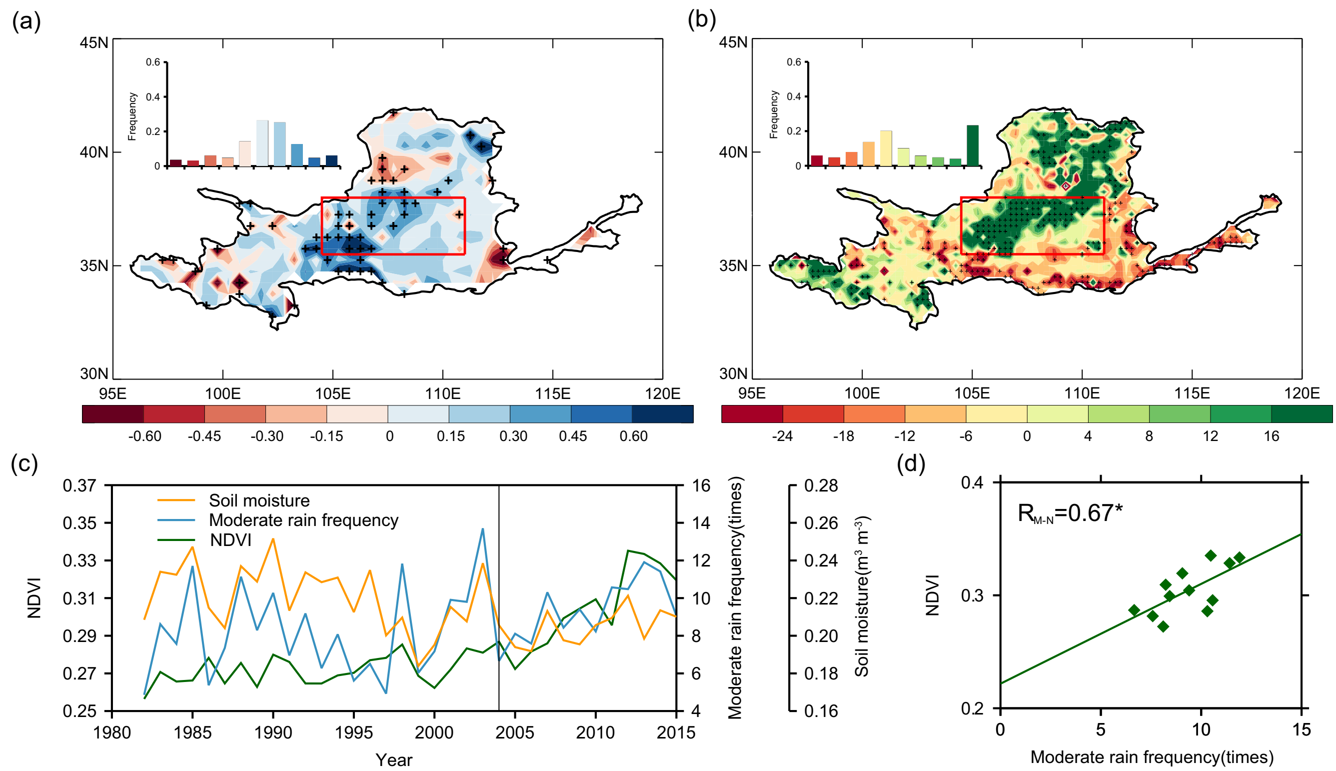

FIGURE 7 Changes of NDVI, moderate rain frequency and soil moisture (0–7 cm) in the central YRB. Spatial distribution of (a) moderate rain frequency trend (units: $times \cdot a^{-1}$), and (b) soil moisture (0–7 cm) trend (units: 10^{-4} $m^3 \cdot m^{-3} \cdot a^{-1}$) after the TP. The small graphs in the upper left corner of (a) and (b) show the frequency distributions of corresponding trends. Stippling indicates passing the significance test ($p < 0.05$). (c) The interannual variations of soil moisture (orange), moderate rain frequency (blue) and NDVI (green) from 1982 to 2015. (d) Correlation between NDVI and moderate rain frequency after the TP. $R_{M\text{-}N}$ is the correlation coefficient (0.67). * indicates passing the significance test ($p < 0.05$). For visual clarity, the black vertical line in (c) is the dividing line with 2004 as the boundary.

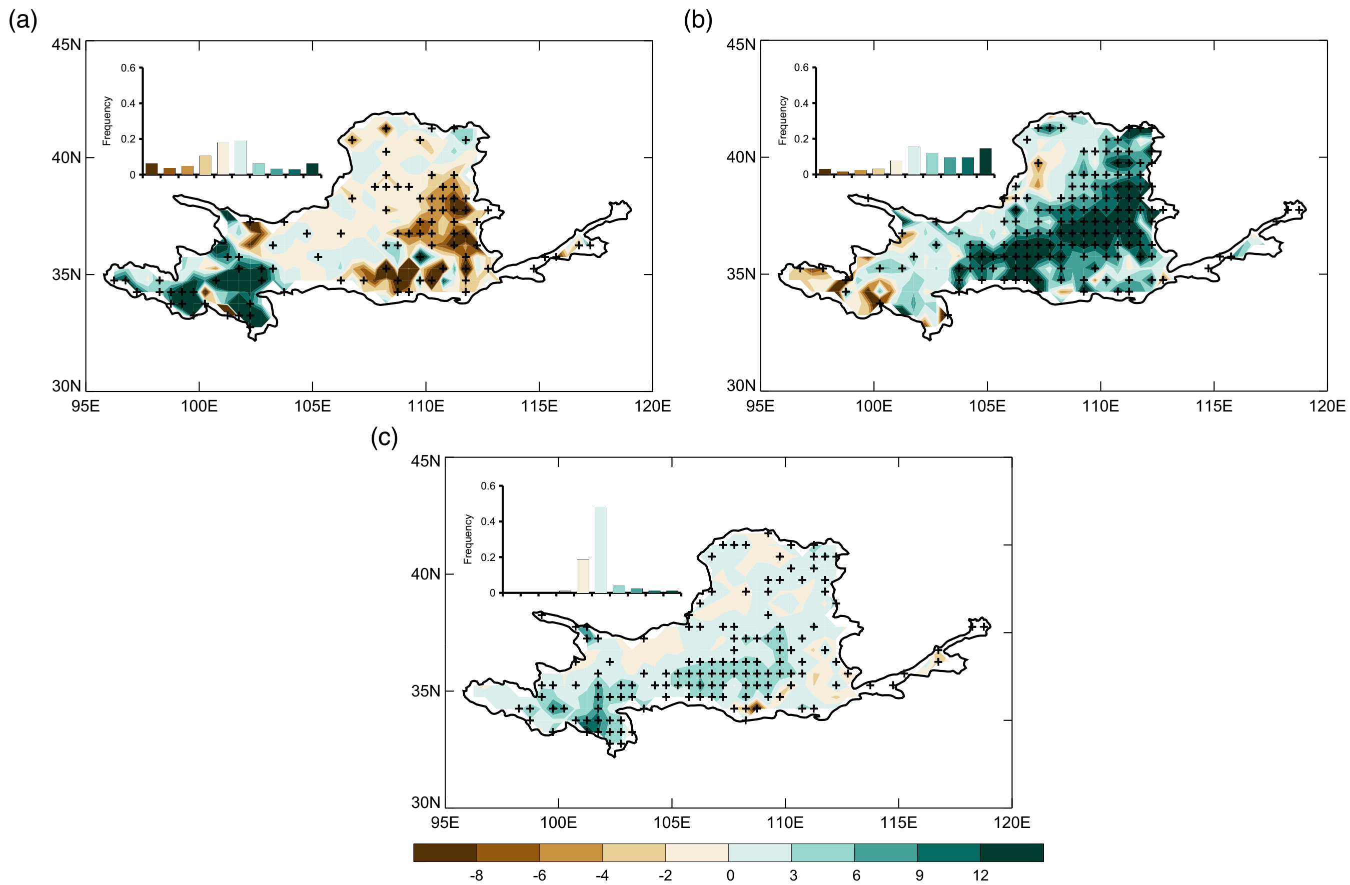

FIGURE 8 Spatial distribution of GPP trend (a) before the TP, (b) after the TP, and (c) during 1982–2015 (units: $gC \cdot m^{-2} \cdot a^{-1}$). The small graphs in the upper left corner show the frequency distributions of corresponding trends. Stippling indicates passing the significance test ($p < 0.05$).

there are 25.9% of the YRB showed a decreasing trend in GPP, with 5.1% exhibiting a significant decrease, distributed in the arid area of the upper reaches, the southeastern part of the middle reaches, and the lower reaches. Before the TP, the GPP in the source region increased rapidly, which trend exceeding more than 12 $gC \cdot m^{-2} \cdot a^{-1}$ (Figure 8a). Except for the source region, 53.0% of the YRB had a decreasing trend in GPP. The arid area of the upper reaches and the lower reaches displayed relatively weak GPP trend (less than −4 $gC \cdot m^{-2} \cdot a^{-1}$), while the decline in the middle reaches was extremely rapid, which reached −8 $gC \cdot m^{-2} \cdot a^{-1}$. After the TP, the ecological enhancement was evident through the rapid growth of GPP in 79.5% of the YRB, predominantly concentrated in the middle and lower reaches (Figure 8b). This observation emphasizes that the TP of the NDVI has a notable effect on GPP. In the central YRB, GPP changed from decreasing before the TP to increasing rapidly, indicating that the ecology was getting better with the recent increase in carbon sequestration capacity.

4 | DISCUSSION

In this study, given that the primary objective is to detect if there is an abrupt change in the trend of the NDVI, and the analysis focuses on a relatively short effective time scale of 26 years (1986–2011), we employed a piecewise linear regression approach with a single TP for the time series of NDVI at each grid point (Equation (1)). And the piecewise linear regression with multiple TPs is commonly applied for the analysis of periodic time series, such as the North Atlantic Oscillation (NAO) (Tomé & Miranda, 2004; Toms & Lesperance, 2003). In other words, if the time series of NDVI have more than one TP, then it suggests significant fluctuations in NDVI during the period of 1982–2015. As demonstrated in Figure 3, the time series of NDVI in the YRB generally exhibited an upward trend and the second TP was calculated to be in 1999. Consequently, selecting one TP suffices for the purpose of detecting the NDVI trend, while selecting multiple TPs is of little significance. Furthermore, the results of the Mann–Kendall test indicate that the TP occurred in the late 20th century, which was consistent with the TP obtained by our piecewise linear regression method (Figure S2 in Supporting Information S1). Although the TP of the Mann–Kendall test did not pass the significance ($p > 0.05$), the result can also prove the accuracy of piecewise linear regression to some extent.

In general, the driving factors for vegetation growth include natural and anthropogenic factors. We conducted a study focusing on natural factors, represented by temperature and precipitation. The increase in NDVI was primarily due to the increased frequency of

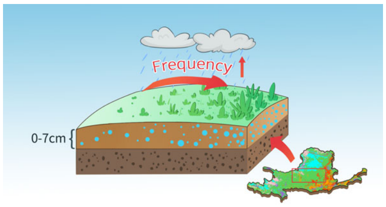

FIGURE 9 Vegetation changes caused by changes in the frequency of moderate rain in the central Yellow River Basin. The small graph in the lower right corner is Figure 1.

moderate rain in the central YRB, leading to an increase in shallow soil moisture content (Figure 9). For the central YRB, the precipitation intensity of light rain is relatively low. Apart from the moisture used for evaporation, the other portion that infiltrates into the soil is too little to effectively promote vegetation growth (Berry & Kulmatiski, 2017; Kulmatiski & Beard, 2013). Although heavy rain brings substantial precipitation, it often leads to surface runoff that cannot be efficiently absorbed by vegetation (Kim et al., 2014). Moderate rain allows more water to infiltrate into the soil without forming surface runoff, facilitating better absorption of moisture by local vegetation. Distinguishing the intensity of precipitation provides an accurate prediction of the relative impact on vegetation growth, offering insights into addressing the challenges of future climate change (Wang et al., 2011). This seems to be a common feature of dryland ecosystems, with moderate rain improving vegetation and ecosystems in both drylands of the western United States and Argentina (Loik et al., 2004; Marone & Pol, 2021).

However, for the other regions in the YRB with diverse ecosystems and complex climatic environments, more detailed investigation is needed. For example, the lower reaches of the YRB are mainly cropland ecosystem and therefore subject to considerable anthropogenic factors. After the TP, the region witnessed a rise in temperature along with a decline in both precipitation and moderate rain frequency. These climatic conditions contributed to a reduction in soil moisture and the NDVI, but an increase of GPP due to fertilization (Hou et al., 2022). While the central YRB comprises a smaller proportion of cropland, it is important to acknowledge the potential impact of irrigation on soil moisture dynamics (Feng et al., 2016). Soil moisture is also affected by other factors than precipitation (Zhao & Dai, 2022). For instance, snowmelt affects soil moisture in the central YRB by contributing 20% of the river discharge (Berg & Sheffield, 2018; Li, Zhang, et al., 2020; Li, Li, et al., 2020; Zhang, Gentine, et al., 2022; Zhang, Li, et al., 2022; Zhang, Piao, et al., 2022). Glacier meltwater also affects soil moisture from July to September by contributing a proportion of river discharge. Nevertheless, since the transition from solid water to liquid water is mainly concentrated in the high-altitude source region with low temperature, its contribution is negligible for the central YRB where there is an absence of snow and glacier. In addition, the temperature of the source region lightly increased but precipitation decreased after the TP, which led to a decline in NDVI and GPP. In summary, the unique climatic conditions in different regions of the YRB resulted in distinct ecological situations. Other studies also indicated that photosynthetically active radiation plays a strong promoting role in vegetation growth by improving photosynthetic efficiency (Yang et al., 2021; Yu et al., 2013). Corresponding to soil moisture, the recent increase in vapour pressure deficit has been shown to inhibit vegetation growth (He et al., 2021; Yuan et al., 2019). Meanwhile, climate change and the rise in carbon dioxide concentration introduce increased uncertainty (Feng et al., 2016). In the lower reaches of the YRB, the recent rapid increase of urbanization contributed substantially to the decreasing trend of the NDVI (Tian et al., 2021; Yuan et al., 2020). In the current scenario of land degradation and expanding desertification, better vegetation management becomes increasingly crucial to drive healthier carbon cycling dynamics (Huang et al., 2016; Wang et al., 2023).

It is important to note that while GPP is widely employed to assess the carbon storage capacity of ecosystems, it does not entirely represent the carbon stored within ecosystems. This is due to the fact that respiration is an equally important process like photosynthesis in the ecosystem, releasing carbon back into the atmosphere. Organisms, including vegetation, animals, and soil microorganisms, undergo autotrophic or heterotrophic respiration, collectively known as total ecosystem respiration (TER), which releases carbon dioxide (Bond-Lamberty et al., 2018). Carbon storage, also known as net ecosystem productivity, is the difference between GPP and TER (Tang et al., 2022). The impact of observed changes in current temperature and precipitation on the net carbon balance of YRB remains unclear. Therefore, in order to estimate the net carbon storage in the YRB, a detailed investigation into the relationship between carbon uptake through photosynthesis and carbon release through respiration is essential.

5 | CONCLUSIONS

We assessed ecological changes over the YRB around the TP in the period of 1982–2015, which promotes our understanding of regional ecological changes in terms of temperature, precipitation and soil moisture. Our study, which predominantly centers on natural factors, underscores an upward trend of the NDVI after the TP was primarily driven by the increase of moderate rain frequency. The increase in moderate rain frequency in the central YRB not only offset the negative impacts of cooling on vegetation growth, but also increased the moisture in the shallow soil layer. The absorbable water of the grassland increased wetting vegetation condition. Although such changes were not strong enough to alter the land type, the GPP in the YRB takes shifted from decreasing to increasing, and resulted in an increase of carbon sequestration capacity in the area.

ACKNOWLEDGEMENTS

This work was supported by the National Natural Science Foundation of China (grant no. 42041004 and 41991231), the "Innovation Star" Project for Outstanding Postgraduates of Gansu Province (grant no. 2023CXZX-105) and the Fundamental Research Funds for the

Central Universities (grant no. lzujbky-2022-ct06). The authors thank the GIMMS group, the ECMWF, the NOAA CPC, the GPCC, the National Qinghai-Tibetan Plateau Data Center, and the RESDC for providing accurate datasets.

CONFLICT OF INTEREST STATEMENT

The authors declare that they have no known competing financial interests or personal relationships that could have appeared to influence the work reported in this paper.

DATA AVAILABILITY STATEMENT

Data are derived from public domain resources. NDVI data was sourced from GIMMS (https://iridl.ldeo.columbia.edu/SOURCES/.NASA/.ARC/.ECOCAST/.GIMMS/.NDVI3g/.v1p0/) group. The 2m air temperature, soil moisture (0-7 cm) data were acquired from the ECMWF ERA5 (https://cds.climate.copernicus.eu/cdsapp#!/dataset/reanalysis-era5-single-levels-monthly-means?tab=form). Precipitation data was obtained from the ECMWF ERA5, the NOAA CPC (https://psl.noaa.gov/data/gridded/data.cpc.globalprecip.html), and the GPCC (https://www.dwd.de/EN/ourservices/gpcc/gpcc.html). GPP data was obtained from the National Qinghai-Tibetan Plateau Data Center (http://data.tpdc.ac.cn/zh-hans/data/d6dff40f-5dbd-4f2d-ac96-55827ab93cc5/?q=gpp). Terrestrial ecosystems data were provided by the RESDC. (https://www.resdc.cn/data.aspx?DATAID=184).

ORCID

Tonghui Gu https://orcid.org/0000-0003-4778-815X

REFERENCES

Angert, A., Biraud, S., Bonfils, C., Henning, C. C., Buermann, W., Pinzon, J., Tucker, C. J., & Fung, I. (2005). Drier summers cancel out the CO_2 uptake enhancement induced by warmer springs. *Proceedings of the National Academy of Sciences*, *102*(31), 10823–10827. https://doi.org/10.1073/pnas.0501647102

Berg, A., & Sheffield, J. (2018). Climate change and drought: The soil moisture perspective. *Current Climate Change Reports*, *4*(2), 180–191. https://doi.org/10.1007/s40641-018-0095-0

Berry, R. S., & Kulmatiski, A. (2017). A savanna response to precipitation intensity[J]. *PLoS One*, *12*(4), e0175402.

Bond-Lamberty, B., Bailey, V. L., Chen, M., Gough, C. M., & Vargas R. (2018). R globally rising soil heterotrophic respiration over recent decades. *Nature*, *560*, 80–83.

Chen, C., Park, T., Wang, X. H., Piao, S. L., Xu, B. D., Chaturvedi, R. K., Fuchs, R., Brovkin, V., Ciais, P., Fensholt, R., Tømmervik, H., Bala, G., Zhu, Z. C., Nemani, R., & Myneni, R. B. (2019). China and India lead in greening of the world through land-use management. *Nature Sustainability*, *2*(2), 122–129. https://doi.org/10.1038/s41893-019-0220-7

Chen, C., Wang, Y. M., Li, Y. Y., & Zhou, S. (2022). Vegetation changes and influencing factors in different climatic regions of Yellow River Basin from 1982 to 2015. *Journal of Yangtze River Scientific Research Institute*, *39*(2), 56–62. https://doi.org/10.11988/ckyyb.20201075

Chen, L., Ma, Z., & Zhao, T. (2016). Modeling and analysis of the potential impacts on regional climate due to vegetation degradation over arid and semi-arid regions of China. *Climatic Change*, *144*(3), 461–473. https://doi.org/10.1007/s10584-016-1847-2

Chen, M. Y., Xie, P. P., Janowiak, J. E., & Arkin, P. A. (2002). Global land precipitation: A 50-yr monthly analysis based on gauge observations. *Journal of Hydrometeorology*, *3*(3), 249–266. https://doi.org/10.1175/1525-7541(2002)003<0249:GLPAYM>2.0.CO;2

Cheng, L., Zhang, L., Wang, Y. P., Canadell, J. G., Chiew, F. H., Beringer, J., Li, L. H., Miralles, D. G., Piao, S. L., & Zhang, Y. Q. (2017). Recent increases in terrestrial carbon uptake at little cost to the water cycle. *Nature Communications*, *8*(1), 1–10. https://doi.org/10.1038/s41467-017-00114-5

Fan, Y., & Van den Dool, H. (2008). A global monthly land surface air temperature analysis for 1948-present. *Journal of Geophysical Research: Atmospheres*, *113*(D1), D01103. https://doi.org/10.1029/2007JD008470

Feng, X. M., Fu, B. J., Piao, S. L., Wang, S., Ciais, P., Zeng, Z. Z., Lv, Y. H., Zeng, Y., Li, Y., Jiang, X. H., & Wu, B. F. (2016). Revegetation in China's loess plateau is approaching sustainable water resource limits. *Nature Climate Change*, *6*, 1019–1022. https://doi.org/10.1038/nclimate3092

Feng, X. M., Fu, B. J., Zhang, Y., Pan, N. Q., Zeng, Z. Z., Tian, H. Q., Lyu, Y., Chen, Y. Z., Ciais, P., Wang, Y. P., Zhang, L., Cheng, L., Maestre, F. T., Fernández-Martínez, M., Sardans, J., & Peñuelas, J. (2021). Recent leveling off of vegetation greenness and primary production reveals the increasing soil water limitations on the greening earth. *Science Bulletin*, *66*(14), 1462–1471. https://doi.org/10.1016/j.scib.2021.02.023

Fensholt, R., Rasmussen, K., Nielsen, T. T., & Mbow, C. (2009). Evaluation of earth observation based long term vegetation trends-Intercomparing NDVI time series trend analysis consistency of Sahel from AVHRR GIMMS, Terra MODIS and SPOT VGT data. *Remote Sensing of Environment*, *113*(9), 1886–1898. https://doi.org/10.1016/j.rse.2009.04.004

Fu, Y. H., Li, X. X., Chen, S. Z., Wu, Z. F., Su, J. R., Li, X., Li, S. F., Zhang, J., Tang, J., & Xiao, J. F. (2022). Soil moisture regulates warming responses of autumn photosynthetic transition dates in subtropical forests. *Global Change Biology*, *28*, 4935–4946. https://doi.org/10.1111/gcb.16227

Fu, Y. H., Piao, S. L., Zhao, H. F., Jeong, S. J., Wang, X. H., Vitasse, Y., Ciais, P., & Janssens, I. A. (2014). Unexpected role of winter precipitation in determining heat requirement for spring vegetation green-up at northern middle and high latitudes. *Global Change Biology*, *20*(12), 3743–3755. https://doi.org/10.1111/gcb.12610

Fu, Y. H., Zhao, H. F., Piao, S. L., Peaucelle, M., Peng, S. S., Zhou, G. Y., Ciais, P., Huang, M. T., Menzel, A., Peñuelas, J., Song, Y., Vitasse, Y., Zeng, Z. Z., & Janssens, I. A. (2015). Declining global warming effects on the phenology of spring leaf unfolding. *Nature*, *526*, 104–107. https://doi.org/10.1038/nature15402

Fu, Y. H., Zhou, X. C., Li, X. X., Zhang, Y. R., Geng, X. J., Hao, F. H., Zhang, X., Hanninen, H., Guo, Y. H., & De Boeck, H. J. (2021). Decreasing control of precipitation on grassland spring phenology in temperate China. *Global Ecology and Biogeography*, *30*, 490–499. https://doi.org/10.1111/geb.13234

Guan, X. D., Ma, J. R., Huang, J. P., Huang, R. X., Zhang, L., & Ma, Z. (2019). Impact of oceans on climate change in drylands. *Science China Earth Sciences*, *62*(6), 891–908. https://doi.org/10.1007/s11430-018-9317-8

Gui, X., Wang, L., & Wang, S. (2021). Environmental factors modulate the diffuse fertilization effect on gross primary productivity across Chinese ecosystems. *Science of the Total Environment*, *793*, 148443. https://doi.org/10.1016/j.scitotenv.2021.148443

He, B., Chen, A. F., Wang, H. L., & Wang, Q. F. (2015). Dynamic response of satellite-derived vegetation growth to climate change in the three north shelter Forest region in China. *Remote Sensing*, *7*, 9998–10016. https://doi.org/10.3390/rs70809998

He, B., Chen, C., Lin, S., Yuan, W., Chen, H. W., Chen, D., Zhang, Y., Guo, L., Zhao, X., Liu, X., Piao, S., Zhong, Z., Wang, R., & Tang, R. (2021). Worldwide impacts of atmospheric vapor pressure deficit on the interannual variability of terrestrial carbon sinks. *National Science Review*, *9*, nwab150.

Hou, H., Zhou, B. B., & Li, X. (2022). Future land use/land cover change has nontrivial and potentially dominant impact on global gross primary productivity. Earth's. *Futures*, *10*(9), e2021EF002628. https://doi.org/10.1029/2021EF002628

Huang, J., Yu, H., Guan, X., Wang, G., & Guo, R. (2016). Accelerated dryland expansion under climate change. *Nature Clim Change*, *6*, 166–171. https://doi.org/10.1038/nclimate2837

Huang, J. P., Zhang, G. L., Yu, H. P., Wang, S. S., Guan, X. D., & Ren, Y. (2020). Characteristics of climate change in the Yellow River basin during recent 40 years. *Shuili Xuebao*, *51*(9), 1048–1058. https://doi.org/10.13243/j.cnki.slxb.20200603

Huang, X. Q., Guan, X. D., Zhu, K. W., Gu, T. H., Huang, J. P., & He, Y. L. (2022). Influence of water vapor influx on interdecadal change in summer precipitation over the source area of the Yellow River Basin. *Atmospheric Research*, *276*, 106270. https://doi.org/10.1016/j.atmosres.2022.106270

Jamali, S., Jönsson, P., Eklundh, L., Ardö, J., & Seaquist, J. (2015). Detecting changes in vegetation trends using time series segmentation. *Remote Sensing of Environment*, *156*, 182–195. https://doi.org/10.1016/j.rse.2014.09.010

Jiang, L. G., Liu, Y., Wu, S., & Yang, C. (2021). Analyzing ecological environment change and associated driving factors in China based on NDVI time series data. *Ecological Indicators*, *129*, 107933. https://doi.org/10.1016/j.ecolind.2021.107933

Jiang, W., Niu, Z., & Ji, Y. (2022). Impacts of drought and climatic factors on vegetation dynamics in the Yellow River Basin and Yangtze River basin, China. *Remote Sensing*, *14*(4), 930. https://doi.org/10.3390/rs14040930

Jiang, W. G., Yuan, L. H., Wang, W. J., Cao, R., Zhang, Y. F., & Shen, W. M. (2014). Spatio-temporal analysis of vegetation variation in the Yellow River Basin. *Ecological Indicators*, *51*, 117–126. https://doi.org/10.1016/j.ecolind.2014.07.031

Kim, J. K., Onda, Y., Kim, M. S., & Yang, D. Y. (2014). Plot-scale study of surface runoff on well-covered forest floors under different canopy species[J]. *Quaternary International*, *344*, 75–85.

Kong, D. D., Zhang, Q., Singh, V. P., & Shi, P. J. (2017). Seasonal vegetation response to climate change in the northern hemisphere (1982–2013). *Global and Planetary Change*, *148*, 1–8. https://doi.org/10.1016/j.gloplacha.2016.10.020

Kong, D. X., Miao, C. Y., Wu, J. W., & Duan, Q. Y. (2016). Impact assessment of climate change and human activities on net runoff in the Yellow River Basin from 1951 to 2012. *Ecological Engineering*, *91*, 566–573. https://doi.org/10.1016/j.ecoleng.2016.02.023

Kulmatiski, A., & Beard, K. (2013). Woody plant encroachment facilitated by increased precipitation intensity. *Nature Clim Change*, *3*, 833–837. https://doi.org/10.1038/nclimate1904

Kumar, S. S., Prihodko, L., Lind, B. M., Anchang, J., Ji, W., Ross, C. W., Kahiu, M. N., Velpuri, N. M., & Hanan, N. P. (2020). Remotely sensed thermal decay rate: An index for vegetation monitoring. *Scientific Reports*, *10*(1), 1–11. https://doi.org/10.1038/s41598-020-66193-5

Lei, Y., Shi, J., Xiong, C., & Ji, D. (2021). Tracking the atmospheric–terrestrial water cycle over the Tibetan Plateau based on ERA5 and grace. *Journal of Climate*, *34*(15), 6459–6471. https://doi.org/10.1175/JCLI-D-20-0692.1

Lenton, T. M., Held, H., Kriegler, E., Hall, J. W., Lucht, W., Rahmstorf, S., & Schellnhuber, H. J. (2008). Tipping elements in the Earth's climate system. *Proceedings of the National Academy of Sciences*, *105*(6), 1786–1793.

Li, C. C., Zhang, Y. Q., Shen, Y. J., & Yu, Q. (2020). Decadal water storage decrease driven by vegetation changes in the Yellow River Basin. *Science Bulletin*, *65*(22), 1859–1861. https://doi.org/10.1016/j.scib.2020.07.020

Li, D., Li, Z., & Lu, X. (2020). Substantial increases in the water and sediment fluxes in the headwater region of the Tibetan plateau in response to global warming. *Geophysical Research Letters*, *47*(11), e2020GL087745. https://doi.org/10.1029/2020GL087745

Li, X., Piao, S., Huntingford, C., Peñuelas, J., Yang, H., Xu, H., & Mahecha, M. D. (2023). Global variations in critical drought thresholds that impact vegetation. *National Science Review*, *10*(5), nwad049.

Liu, H. P., & Randerson, J. T. (2008). Interannual variability of surface energy exchange depends on stand age in a boreal forest fire chronosequence. *Journal of Geophysical Research: Biogeosciences*, *113*(G1), G01006. https://doi.org/10.1029/2007JG000483

Liu, H. P., Randerson, J. T., Lindfors, J., & Chapin, F. S., III. (2005). Changes in the surface energy budget after fire in boreal ecosystems of interior Alaska: An annual perspective. *Journal of Geophysical Research: Atmospheres*, *110*(D13), D13101. https://doi.org/10.1029/2004JD005158

Liu, H. Y., Jiao, F. S., Gong, H. B., Wang, Z. Y., & Lin, Z. S. (2019). Nonlinear relationship of vegetation greening with nature and human factors and its forecast: A case study of Southwest China. *Ecological Indicators*, *111*, 106009. https://doi.org/10.1016/j.ecolind.2019.106009

Liu, M., Gao, Y., Wei, H., Dong, X., Zhao, B., Wang, X. C., Zhang, P., Liu, R., & Zou, X. (2022). Profoundly entwined ecosystem services, land-use change and human well-being into sustainability management in Yushu, Qinghai-Tibet plateau. *Journal of Geographical Sciences*, *32*(9), 1745–1765.

Liu, T., Chen, D., Yang, L., Meng, J., Wang, Z., Ludescher, J., Fan, J., Yang, S., Chen, D., Kurths, J., Chen, X., Havlin, S., & Schellnhuber, H. J. (2023). Teleconnections among tipping elements in the earth system. *Nature Climate Change*, *13*(1), 67–74.

Loik, M. E., Breshears, D. D., Lauenroth, W. K., & Belnap, J. (2004). A multi-scale perspective of water pulses in dryland ecosystems: Climatology and ecohydrology of the western USA. *Oecologia*, *141*(2), 269–281. https://doi.org/10.1007/s00442-004-1570-y

Lu, N., Tian, H. P., Fu, B. J., Yu, H. Q., Piao, S. L., Chen, S. Y., Li, Y., Li, X. Y., Wang, M. Y., Li, Z. D., Zhang, L., Ciais, P., & Smith, P. (2022). Biophysical and economic constraints on China's natural climate solutions. *Nature Climate Change*, *12*, 847–853. https://doi.org/10.1038/s41558-022-01432-3

Ma, Z. G., Fu, C. B., Zhou, T. J., Yan, Z. W., Li, M. X., Zheng, Z. Y., Chen, L., & Lv, M. X. (2020). Status and ponder of climate and hydrology changes in the Yellow River Basin. *Bulletin of the Chinese Academy of Sciences*, *35*(1), 52–60. https://doi.org/10.16418/j.issn.1000-3045.20191223002

Marone, L., & Pol, R. G. (2021). Continuous grazing disrupts desert grass-soil seed bank composition under variable rainfall. *Plant Ecology*, *222*, 247–259. https://doi.org/10.1007/s11258-020-01102-4

Myneni, R. B., Keeling, C. D., Tucker, C. J., Asrar, G., & Nemani, R. R. (1997). Increased plant growth in the northern high latitudes from 1981 to 1991. *Nature*, *386*, 698–702. https://doi.org/10.1038/386698a0

Nemani, R. R., Keeling, C. D., Hashimoto, H., Jolly, W. M., Piper, S. C., Tucker, C. J., Myneni, R. B., & Running, S. W. (2003). Climate-driven increases in global terrestrial net primary production from 1982 to 1999. *Science*, *300*, 1560–1563. https://doi.org/10.1126/science.1082750

Niu, Y. L., Li, S. Y., & Wu, G. L. (2021). Regulation of alpine meadow patch coverage on runoff and sediment under natural rainfall on the eastern Qinghai-Tibetan plateau. *Journal of Hydrology*, *603*, 127101. https://doi.org/10.1016/j.jhydrol.2021.127101

Pang, G., Wang, X., Chen, D., Yang, M., & Liu, L. (2021). Evaluation of a climate simulation over the Yellow River Basin based on a regional climate model (REMO) within the CORDEX. *Atmospheric Research*, *254*, 105522. https://doi.org/10.1016/j.atmosres.2021.105522

Peng, S. S., Piao, S., Zeng, Z., Ciais, P., Zhou, L., Li, L. Z. X., Myneni, R. B., Yin, Y., & Zeng, H. (2014). Afforestation in China cools local land surface temperature. *Proceedings of the National Academy of Sciences*, *111*(8), 2915–2919. https://doi.org/10.1073/pnas.1315126111

Piao, S. L., Fang, J. Y., Ciais, P., Peylin, P., Huang, Y., Sitch, S., & Wang, T. (2009). The carbon balance of terrestrial ecosystems in China. *Nature*, *458*, 1009–1013. https://doi.org/10.1038/nature07944

Piao, S. L., Wang, X. H., Park, T., Chen, C., Lian, X., He, Y., Bjerke, J. W., Chen, A. P., Ciais, P., Tømmervik, H., Nemani, R. R., & Myneni, R. B. (2020). Characteristics, drivers and feedbacks of global greening. *Nature Reviews Earth & Environment*, *1*(1), 14–27. https://doi.org/10.1038/s43017-019-0001-x

Piao, S., Yin, G., Tan, J., Cheng, L., Huang, M., Li, Y., Liu, R., Mao, J., Myneni, R. B., Peng, S., Poulter, B., Shi, X., Xiao, Z., Zeng, N., Zeng, Z., & Wang, Y. (2011). Changes in satellite-derived vegetation growth trend in temperate and boreal Eurasia from 1982 to 2006. *Global change biology*, *17*(10), 3228–3239. https://doi.org/10.1111/gcb.12795

Piao, S. L., Yin, G. D., Tan, J. G., Cheng, L., Huang, M. T., Li, Y., Liu, R. G., Mao, J. F., Myneni, R. B., Peng, S. S., Poulter, B., Shi, X. Y., Xiao, Z. Q., Zeng, N., Zeng, Z. Z., & Wang, Y. P. (2015). Detection and attribution of vegetation greening trend in China over the last 30 years. *Global Change Biology*, *21*, 1601–1609. https://doi.org/10.1111/gcb.12795

Shea, E. K., & Vecchione, M. (2002). Quantification of ontogenetic discontinuities in three species of oegopsid squids using model II piecewise linear regression. *Marine Biology*, *140*(5), 971–979. https://doi.org/10.1007/s00227-001-0772-7

Shi, Y. F., Shen, Y. P., Li, D. L., Zhang, G. W., Ding, Y. J., Hu, R. J., & Kang, E. S. (2003). Discussion on the present climate change from warm-day to warm-wet in Northwest China, *23*(2), 152–164. https://doi.org/10.3321/j.issn:1001-7410.2003.02.005

Song, X. D., Wu, H. Y., Ju, B., Liu, F., Yang, F., Li, D. C., Zhao, Y. G., Yang, J. L., & Zhang, G. L. (2020). Pedoclimatic zone-based three-dimensional soil organic carbon map** in China. *Geoderma*, *363*, 114145.

Sun, R., Chen, S. H., & Su, H. B. (2021). Climate dynamics of the spatiotemporal changes of vegetation NDVI in northern China from 1982 to 2015. *Remote Sensing*, *13*(2), 187. https://doi.org/10.3390/rs13020187

Tang, R., He, B., & Yang, Y. (2022). Increasing terrestrial ecosystem carbon release in response to autumn cooling and warming. *Nature Climate Change*, *12*(4), 380–385. https://doi.org/10.1038/s41558-022-01304-w

Tian, F., Liu, L. Z., Yang, J. H., & Wu, J. J. (2021). Vegetation greening in more than 94% of the Yellow River Basin (YRB) region in China during the 21st century caused jointly by warming and anthropogenic activities. *Ecological Indicators*, *125*(2), 107479. https://doi.org/10.1016/j.ecolind.2021.107479

Tomé, A. R., & Miranda, P. M. A. (2004). Piecewise linear fitting and trend changing points of climate parameters. *Geophysical Research Letters*, *31*(2), L02207. https://doi.org/10.1029/2003GL019100

Toms, J. D., & Lesperance, M. L. (2003). Piecewise regression: A tool for identifying ecological thresholds. *Ecology*, *84*(8), 2034–2041. https://doi.org/10.1890/02-0472

Tucker, C. J., Pinzon, J. E., Brown, M. E., Slayback, D. A., Pak, E. W., Mahoney, R., Vermote, E. F., & El Saleous, N. (2005). An extended AVHRR 8-km NDVI dataset compatible with MODIS and SPOT vegetation NDVI data. *International Journal of Remote Sensing*, *26*(20), 4485–4498. https://doi.org/10.1080/01431160500168686

Ukkola, A. M., De Kauwe, M. G., Roderick, M. L., Burrell, A., Lehmann, P., & Pitman, A. J. (2021). Annual precipitation explains variability in dryland vegetation greenness globally but not locally. *Global Change Biology*, *27*(18), 4367–4380. https://doi.org/10.1111/gcb.15729

Wang, S., Fu, B., Wei, F., Piao, S., Maestre, F. T., Wang, L., Jiao, W., Liu, Y., Li, Y., Li, C., & Zhao, W. (2023). Drylands contribute disproportionately to observed global productivity increases. *Science Bulletin*, *68*(2), 224–232.

Wang, S. H., Zhang, Y. G., Ju, W. M., Qiu, B., & Zhang, Z. Y. (2021). Tracking the seasonal and inter-annual variations of global gross primary production during last four decades using satellite near-infrared reflectance data. *Science of the Total Environment*, *755*, 142569. https://doi.org/10.1016/j.scitotenv.2020.142569

Wang, S. P., Wang, Z. H., Piao, S. L., & Fang, J. Y. (2010). Regional differences in the timing of recent air warming during the past four decades in China. *Chinese Science Bulletin*, *55*(19), 1968–1973. https://doi.org/10.1007/s11434-010-3236-y

Wang, X. H., Piao, S. L., Ciais, P., Li, J. S., Friedlingstein, P., Koven, C., & Chen, A. P. (2011). Spring temperature change and its implication in the change of vegetation growth in North America from 1982 to 2006. *Proceedings of the National Academy of Sciences*, *108*(4), 1240–1245. https://doi.org/10.1073/pnas.1014425108

Wei, Y., Lu, H., & Sun, J. (2022). Dual influence of climate change and anthropogenic activities on the spatiotemporal vegetation dynamics over the Qinghai-Tibetan plateau from 1981 to 2015. Earth's. *Futures*, *10*(5), e2021EF002566. https://doi.org/10.1029/2021EF002566

Weisberg, S. (2005). *Applied linear regression* (Vol. 528, pp. 19–68). John Wiley & Sons.

Xi, J. P. (2019). Speech at a symposium on ecological protection and high-quality development in the Yellow River Basin. *Water Conservancy Construction and Management*, *39*(11), 1–3, 6. https://doi.org/10.16616/j.cnki.11-4446/TV.2019.11.01

Xin, Z. B., Xu, J. X., & Zheng, W. (2008). Spatiotemporal variations of vegetation cover on the Chinese loess plateau (1981-2006): Impacts of climate changes and human activities. *Science in China Series D: Earth Sciences*, *51*(1), 67–78. https://doi.org/10.1007/s11430-007-0137-2

Xu, H. J., & Yang, T. B. (2014). Spatial-temporal variations of vegetation activities and its responses to climatic factors in the Qaidam Basin. *Journal of Natural Resources*, *29*(3), 398–409. https://doi.org/10.11849/zrzyxb.2014.03.004

Xu, L., Myneni, R. B., Chapin, F. S., III, Callaghan, T. V., Pinzon, J. E., Tucker, C. J., Zhu, P., Bi, J., Ciais, P., Tømmervik, H., Euskirchen, E. S., Forbes, B. C., Piao, S. L., Anderson, B. T., Ganguly, S., Nemani, R. R., Goetz, S. J., Beck, P. S. A., Bunn, A. G., … Stroeve, J. C. (2013). Temperature and vegetation seasonality diminishment over northern lands. *Nature Climate Change*, *3*(6), 581–586. https://doi.org/10.1038/nclimate1836

Yang, D. W., Yang, Y. T., & Xia, J. (2021). Hydrological cycle and water resources in a changing world: A review. *Geography and Sustainability*, *2*(2), 115–122. https://doi.org/10.1016/j.geosus.2021.05.003

Yang, Y. T., Guan, H. D., Batelaan, O., McVicar, T. R., Long, D., Piao, S. L., Liang, W., Liu, B., Jin, Z., & Simmons, C. T. (2016). Contrasting responses of water use efficiency to drought across global terrestrial ecosystems. *Scientific Reports*, *6*(1), 1–8. https://doi.org/10.1038/srep23284

Yao, J., Mao, W., Chen, J., & Dilinuer, T. (2021). Recent signal and impact of wet-to-dry climatic shift in Xinjiang, China. *Journal of Geographical Sciences*, *31*, 1283–1298.

Yao, J. Y., Gao, Z. M., Huang, J. P., Liu, H. P., & Wang, G. Y. (2021). Technical note: Uncertainties in eddy covariance CO_2 fluxes in a semiarid sagebrush ecosystem caused by gap-filling approaches. *Atmospheric Chemistry and Physics*, *21*(20), 15589–15603. https://doi.org/10.5194/acp-21-15589-2021

Yao, J. Y., Liu, H. P., Huang, J. P., Gao, Z. M., Wang, G. Y., Li, D., Yu, H. P., & Chen, X. Y. (2020). Accelerated dryland expansion regulates future variability in dryland gross primary production. *Nature Communications*, *11*(1665), 1–10. https://doi.org/10.1038/s41467-020-15515-2

Yao, R., Wang, L. C., Huang, X., Chen, X. X., & Liu, Z. J. (2019). Increased spatial heterogeneity in vegetation greenness due to vegetation greening in mainland China. *Ecological Indicators*, *99*, 240–250. https://doi.org/10.1016/j.ecolind.2018.12.039

Yu, X. L., Wu, Z. C., & Guo, X. L. (2013). Investigating the potential of GIMMS and MODIS NDVI data sets for estimating gross primary productivity in Harvard Forest. *International workshop on analysis of multi-temporal remote sensing images*, IEEE. https://doi.org/10.1109/Multi-Temp.2013.6866013

Yu, Z., Ciais, P., Piao, S. L., & Zhou, G. (2022). Forest expansion dominates China's land carbon sink since 1980. *Nature Communications*, *13*(1), 5374. https://doi.org/10.1038/s41467-022-32961-2

Yuan, M. X., Wang, L. C., Lin, A. W., Liu, Z. J., Li, Q. J., & Qu, S. (2020). Vegetation green up under the influence of daily minimum temperature and urbanization in the Yellow River Basin, China. *Ecological Indicators*, *108*, 105760. https://doi.org/10.1016/j.ecolind.2019.105760

Yuan, W. P., Lin, S. R., & Wang, X. Y. (2022). Progress of studies on satellite-based terrestrial vegetation production models in China. *Progress in Physical Geography: Earth and Environment*, *46*, 889–908. https://doi.org/10.1177/03091333221114864

Yuan, W. P., Zheng, Y., Piao, S. L., Ciais, P., Lombardozzi, D., Wang, Y. P., Ryu, Y., Chen, G. X., Dong, W. J., Hu, Z. M., Jain, A. K., Jiang, C. Y., Kato, E., Li, S. H., Lienert, S., Liu, S. G., Nable, J. E. M. S., Qin, Z. C., Quine, T., … Yang, S. (2019). Increased atmospheric vapor pressure deficit reduces global vegetation growth. *Science*. *Advances*, *5*(8), eaax1396. https://doi.org/10.1126/sciadv.aax1396

Zhang, T., Li, D., & Lu, X. (2022). Response of runoff components to climate change in the source-region of the Yellow River on the Tibetan plateau. *Hydrological Processes*, *36*(6), e14633. https://doi.org/10.1002/hyp.14633

Zhang, X. B., & Liu, L. X. (2020). Study on the change characteristics of water resources in the Yellow River Basin from 1998 to 2018. *Ground Water*, *42*(5), 187–189. https://doi.org/10.19807/j.cnki.DXS.2020-05-058

Zhang, Y., Gentine, P., & Keenan, T. F. (2022). Increasing sensitivity of dryland vegetation greenness to precipitation due to rising atmospheric CO^2. *Nature Communications*, *13*(1), 4875. https://doi.org/10.1038/s41467-022-32631-3

Zhang, Y. C., Piao, S. L., & Peñuelas, J. (2022). Future reversal of warming-enhanced vegetation productivity in the northern hemisphere. *Nature Climate Change*, *12*(6), 581–586. https://doi.org/10.1038/s41558-022-01374-w

Zhao, A. Z., Zhang, A. B., Feng, L. L., Wang, D. L., & Cheng, D. Y. (2019). Spatio-temporal characteristics of water-use efficiency and its relationship with climatic factors in the Haihe River basin. *Acta Ecologica Sinica*, *39*(4), 1452–1462. https://doi.org/10.5846/stxb201810072158

Zhao, H. F., Fu, Y. H., Wang, X. H., Zhang, Y., Liu, Y. W., & Janssens, I. A. (2020). Diverging models introduce large uncertainty in future climate warming impact on spring phenology of temperate deciduous trees. *Science of the Total Environment*, *757*, 143903. https://doi.org/10.1016/j.scitotenv.2020.143903

Zhao, T., & Dai, A. (2022). CMIP6 model-projected Hydroclimatic and drought changes and their causes in the twenty-first century. *Journal of Climate*, *35*, 897–921. https://doi.org/10.1175/JCLI-D-21-0442.1

Zhou, S., Zhang, Y., & Gentine, P. (2019). Projected increases in intensity, frequency, and terrestrial carbon costs of compound drought and aridity events. Science. *Advances*, *5*(1), eaau5740. https://doi.org/10.1126/sciadv.aau5740

Zhu, K. W., Guan, X. D., Huang, J. P., Wang, J. M., Guo, S. Y., & Cao, C. Y. (2021). Precipitation over semi-arid regions of north hemisphere affected by Atlantic multidecadal oscillation. *Atmospheric Research*, *262*, 105801. https://doi.org/10.1016/j.atmosres.2021.105801

Zhu, X. F., Xiao, G. F., Zhang, D. J., & Guo, L. (2021). Mapping abandoned farmland in China using time series MODIS NDVI. *Science of the Total Environment*, *755*, 142651.

SUPPORTING INFORMATION

Additional supporting information can be found online in the Supporting Information section at the end of this article.

How to cite this article: Gu, T., Guan, X., Huang, J., Shen, X., Huang, X., Zhang, G., Han, D., Fu, L., & Nie, J. (2023). The turning of ecological change in the Yellow River Basin. *Hydrological Processes*, *37*(12), e15055. https://doi.org/10.1002/hyp.15055